European Radiology (2019) 29:6671–6681
https://doi.org/10.1007/s00330-019-06283-9

MAGNETIC RESONANCE

Differentiation of human cartilage degeneration by functional MRI mapping—an ex vivo study

Daniel Truhn[1] · Björn Sondern[1] · Simon Oehrl[1] · Markus Tingart[2] · Matthias Knobe[3] · Dorit Merhof[4] · Christiane Kuhl[1] · Johannes Thüring[1] · Sven Nebelung[1]

Received: 5 November 2018 / Revised: 25 April 2019 / Accepted: 22 May 2019 / Published online: 11 June 2019

Abstract

Objective To evaluate whether the response to loading of cartilage samples as assessed ex vivo by quantitative MRI (qMRI) mapping techniques can differentiate intact and early degenerative cartilage.

Methods Upon IRB approval and written informed consent, 59 macroscopically intact osteochondral samples were obtained from the central lateral femoral condyles of patients undergoing total knee replacement. Spatially resolved T1, T2, T2*, and T1ρ maps were generated prior to and during displacement-controlled quasi-static indentation loading to 405 μm ($\Delta_{1/2}$) and 810 μm (Δ_1). Upon manual segmentation, absolute qMRI parameters and loading-induced relative changes ($\delta_{1/2}$, δ_1) were determined for the entire cartilage sample and distinct zones and regions. Based on their histologically determined degeneration as quantified according to Mankin (Mankin sum scores [MSS], range 0–14), samples were dichotomised into intact (*int*; MSS 0–4, $n = 35$) and early degenerative (*ed*, MSS 5–8, $n = 24$).

Results For T1ρ, consistent loading-induced increases were found for $\delta_{1/2}$ and δ_1. Throughout the entire sample, increases in T1ρ were significantly higher in early degenerative than in intact samples ($\Delta_{1/2}(ed) = 23.8$ [$q_{25} = 18.1$, $q_{75} = 29.0$] %; $\Delta_{1/2}(int) = 12.7$ [$q_{25} = 5.9$, $q_{75} = 19.5$] %; $p < 0.0005$), according to Wilcoxon's signed-rank test). Zonal and regional analysis revealed these changes to be most pronounced in the sub-pistonal area. No significant degeneration-dependent loading-induced changes were found for T1, T2, or T2*.

Conclusion Aberrant load-bearing of early degenerative cartilage may be detected using T1ρ mapping as a function of loading. Hence, the diagnostic differentiation of intact versus early degenerative cartilage may allow the reliable identification of early and potentially reversible cartilage degeneration, thereby opening new opportunities for diagnosis and treatment of cartilage pathologies.

Electronic supplementary material The online version of this article (https://doi.org/10.1007/s00330-019-06283-9) contains supplementary material, which is available to authorized users.

✉ Daniel Truhn
dtruhn@ukaachen.de

[1] Department of Diagnostic and Interventional Radiology, Aachen University Hospital, Aachen, Germany

[2] Department of Orthopaedics, Aachen University Hospital, Aachen, Germany

[3] Department of Trauma Surgery, Aachen University Hospital, Aachen, Germany

[4] Institute of Imaging and Computer Vision, RWTH Aachen, Aachen, Germany

Key Points

- *T1ρ mapping of the cartilage response to loading allows the reliable identification of early degenerative changes ex vivo.*
- *Distinct response-to-loading patterns of cartilage tissue as assessed by functional MRI techniques are associated with biomechanical and histological tissue properties.*
- *Non-invasive functional MR imaging techniques may facilitate the more sensitive monitoring of therapeutic outcomes and treatment strategies.*

Keywords Magnetic resonance imaging · Cartilage · Knee joint

Abbreviations

δ_x	Indentation position *x*
$\Delta\delta_x$	Relative change of MRI parameter at indentation position *x*
ρ	Spearman's correlation coefficient
DZ	Deep zone
ECS	Entire cartilage sample
ed	Early degenerative
FT	Full thickness
int	Intact
IYM	Instantaneous Young's modulus
KL	Kellgren-Lawrence grade
MSS	Mankin sum score
OA	Osteoarthritis
PPA	Peri-pistonal area
SPA	Sub-pistonal area
SZ	Superficial zone
TZ	Transitional zone

Introduction

Early identification of osteoarthritis (OA) is of utmost importance as preventive measures may halt or slow its progression [1]. Even though advanced stages of OA can be detected by routine clinical imaging tools, they lack the ability to detect early stages of OA [2, 3], which are characterised by distinct degenerative cartilage changes such as proteoglycan depletion, increased intra-tissue water content, and loss of collagen fibre orientation, thereby reducing resistance to loading [4]. Hence, the depiction of compositional intra-tissue changes and the assessment of cartilage softening offer potential diagnostic targets for the non-invasive detection of early cartilage changes.

Recent scientific efforts have employed quantitative MR imaging (qMRI) techniques to gain insights into the distribution of the extracellular matrix component water, collagen, and proteoglycans [2, 5]. Despite promising results (excellently reviewed in [6]), consistently detecting slight changes was hindered by the qMRI parameters' large intra- and inter-individual variability, which does not allow the reliable differentiation of intact versus early degenerative cartilage, neither by T2 nor by T1ρ mapping [5, 7]. It is against this background that additional biomechanical stimuli have been implemented within MRI protocols. Several studies have investigated the response to loading of human articular cartilage ex vivo [6, 8, 9] and in vivo [10–12] in efforts to reliably detect cartilage softening as a surrogate marker of early cartilage degeneration.

Early studies on T1ρ and T2 have indicated that the tissue's functionality was significantly altered in patients with radiographic evidence of OA [10, 13]. Investigating loading-induced changes in non-OA versus OA patients (defined as no radiographic evidence of OA [i.e. Kellgren-Lawrence scores (KL) ≤ 1] vs. its definite presence [i.e. KL > 1]), Souza et al found loading-induced changes in T1ρ and T2 to be larger in OA patients suggesting altered load-bearing [10]. Limitations involve inconsistencies in loading protocols and shortfalls in cohort sizes and reference evaluation. Referencing is highly relevant as cohort allocation (OA vs. non-OA) was performed through conventional radiography, which is a coarse evaluation tool with limited sensitivity, correlation with histology, and differentiation of degeneration [2].

As the histologic assessment undoubtedly represents the reference standard, our study's purpose was to evaluate whether the cartilage response to loading as assessed by qMRI mapping techniques can differentiate intact and early degenerative cartilage. We hypothesised that loading-induced changes in qMRI parameters were related to the histological grade of degeneration in human articular cartilage, thereby allowing the above-mentioned differentiation.

Materials and methods

Study design

The study was set up as an intra-individual comparative prospective ex vivo imaging study of human cartilage samples. Cartilage samples were obtained from patients undergoing total knee replacements at our institution. Local Institutional Review Board approval (Ethical Committee, RWTH Aachen, Germany, AZ-EK157/13) and individual written informed patient consent were obtained prior to the study.

Sample size estimation

The sample size was calculated based on a two-sample *t* test and corrected for the use of the non-parametric Wilcoxon signed-rank test. Based on an earlier comparable study, a one-sided hypothesis was tested [1]. Employing an effect size of 0.7, a statistical power of 0.8, and an alpha error of 0.05, a minimum sample size of 26 for each group was calculated based on the *t* test, i.e. a total sample size of 52 (assuming equally sized groups). As the testing design was non-parametric, the calculated sample size needed to be adjusted by the asymptotic relative efficiency of the non-parametric Wilcoxon signed-rank test, i.e. 95.5%, rendering the minimal sample size to 55.

Preparation of cartilage samples

As before [14, 15], cartilage-bone material was included only in cases of primary osteoarthritis involving at least the medial joint compartment, while secondary OA and other bone and joint disorders (e.g. rheumatoid arthritis) as well as a history of trauma or surgery to the knee were defined as exclusion criteria. Sample preparation steps were as follows: The cartilage-bone material that had been excised during surgery was transferred to the sterile cell culture medium (Dulbecco's modified Eagle's medium, Gibco-BRL) and kept refrigerated at 4 °C. In keeping with the study's purpose, macroscopically intact, grossly intact, and slightly altered cartilage areas from the central part of the lateral femoral condyle were selected upon macroscopic evaluation by the senior author (SN) so that samples with macroscopic Outerbridge grades 0 (intact), 1 (softening, swelling), and 2 (partial-thickness tissue alterations) were included. Due to the Outerbridge classification's limitations [16], sample status was ultimately based on histology. Samples were cut to standard size (20 mm × 20 mm; width × length) and any cancellous bone was trimmed, while the subchondral lamella was preserved to prevent bone compaction during loading. For reference, the mid-sagittal plane was defined by creating two notches at opposing sample sides using a rongeur, while a third notch defined the sample centre as the intersection between the mid-sagittal and the orthogonal plane.

MRI measurements

MRI examinations were performed on a clinical 3.0-T MRI scanner (Achieva, Philips) within 24 h following sample preparation using a modified single-channel prostate coil (BPX-30, Medrad). Samples were imaged in the unloaded (δ_0) and loaded states ($\delta_{1/2}$, δ_1) using a dedicated MRI-compatible indentation loading device [14] that had been thoroughly validated before [17]. From the initial contact point, defined as the first contact between the indentor piston and sample surface, a 180° drive rod rotation brought about uniaxial displacement of 405 μm (connoted by $\delta_{1/2}$) which resulted in a mean strain of 20.3 ± 5.4% based on sample thickness (as determined histologically). Consequently, a full 360° drive rod rotation induced uniaxial displacement of 810 μm (δ_1) and mean strains of 40.5% ± 10.7%. The details of the sample-loaded indentation device are given in Fig. 1.

The imaging plane was defined as the central dissecting plane along the mid-sagittal plane. Subsequently, spatial mapping of T2*, T2, T1ρ, and T1 relaxation was performed in this order using the sequences as detailed in Table 1. Total imaging time per sample and indentation position was 37 min. An equilibration period of 5 min was observed after loading to each displacement step before the measurements were initiated. Samples were imaged at room temperature which was monitored at the beginning and at the end of the measurements (20.2 ± 0.6 °C).

Data processing

The MR raw data and respective time constants for each pixel of the mid-sagittal image were imported into Matlab (MatlabR2017b) and quantitative T1, T1ρ, T2, and T2* maps were generated using established mono-exponential fitting routines [14, 18]. Fit quality was checked using R^2 statistics adjusted to the degrees of freedom (threshold, $R^2 \geq 0.95$). Manual segmentation of the cartilage sample outlines was performed for each indentation level separately based on the morphological images (TE = 24 ms) by choosing pixels laying safely within the tissue to avoid partial volume effects at the top- and bottom-most layers (towards medium/piston and subchondral lamella). Manual segmentation was performed by one author (SO / 3 years of experience) and checked by two experienced radiologists, i.e. both the first (DT, 6 years of experience) and the last author (SN, 6 years of experience). Segmentation outlines were transferred to the parameter maps using scanner coordinates and checked by visual comparison. Alongside the entire cartilage sample (ECS), tissue regions were defined as the sub-pistonal area (SPA, i.e. the tissue region underneath the indentor piston, 6 mm width) and the peri-pistonal area (PPA, i.e. the adjacent tissue regions). The cartilage thickness was zonally stratified into the superficial zone (SZ), transitional zone (TZ), and deep zone (DZ), comprising 0–15%, 15–65%, and 65–100% of total cartilage thickness and the full-thickness zone (FT, 0–100%).

Reference evaluations

Within 12 h of the MR measurements, the samples underwent reference evaluation in terms of biomechanical testing and histologic analyses. Of note, a detailed description of the biomechanical and histologic methods is available online (Online Supplement 1). Briefly, cylindrical cartilage samples were prepared from the sample centre region to undergo unconfined

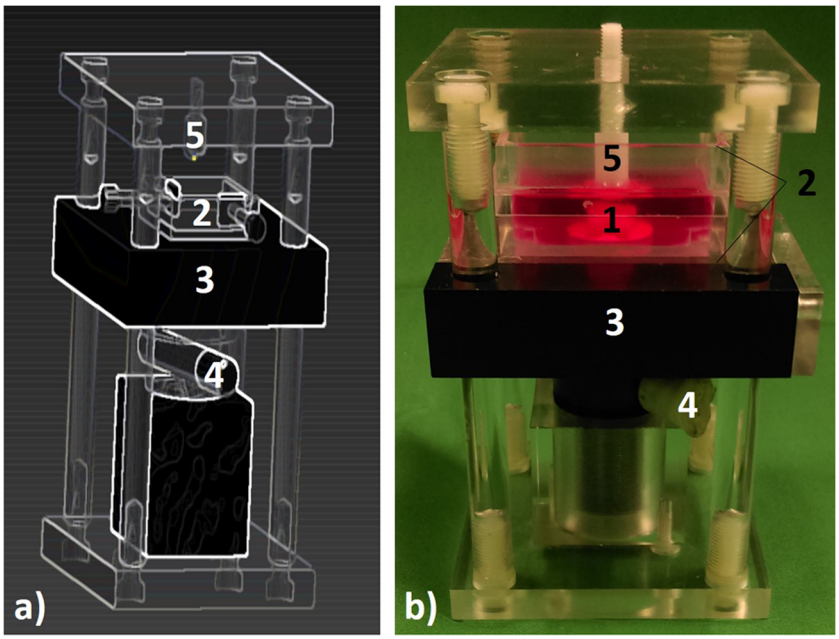

Fig. 1 Measurement setup. Rendered CAD image with edge enhancement (**a**) and photograph (**b**) of the MRI-compatible displacement-controlled indentation loading device. The cartilage sample (1, not shown in **a**) is positioned within the medium-filled sample container (2) positioned on top of the centred base plate (3) which is controlled by a drive rod (4), which displaced the centre plate upwards towards the indenter piston (5) to thereby induced indentation loading of the cartilage sample

compression loading to determine the sample's instantaneous Young modulus. To obtain histological sections that were as representative of the sample in its entirety as possible, osteochondral regions directly adjacent to this centre region were harvested for histological analyses in line with standard protocols. Following staining with haematoxylin/eosin and Safranin O, sections were assessed by three blinded investigators experienced in musculoskeletal histopathology (SN [9 years of experience], BS [5 years], DT [4 years]) using the Mankin classification [19] to determine the Mankin sum scores (MSS, range 0–14 with 0/14 indicating no/most severe degeneration). Based thereon, sample allocation was dichotomised to the intact (int, MSS, 0–4) or early degenerative subgroup (ed, MSS 5–8) [19, 20]. After initial individual assessment, any differences in the initial scores were discussed until consensus was reached. Mean sample thickness was determined using the in-built calliper function of Diskus software (Leica) by measuring the vertical from the cartilage surface to the cartilage-bone transition at the centre point and two positions at ± 2.0 mm to either side.

Table 1 Acquisition parameters of MR sequences

	T1	T1ρ	T2	T2*
Sequence type	Inversion recovery	Spin-lock multi-gradient echo	Multi-spin echo	Multi-gradient echo
Repetition time (ms)	3000	30	1500	700
Echo time (ms)	10.1	3.83	$n \times 8.38$ ($n = 1$–12)	$3.34 + n \times 5.2$ ($n = 0$–15)
Turbo spin echo factor	5	44	12	15
Field of view (mm)	62 × 62	52 × 52	52 × 52	52 × 52
Acquisition matrix	224 × 220	176 × 176	176 × 176	176 × 176
Reconstruction matrix	224 × 220	176 × 176	176 × 176	176 × 176
Flip angle (°)	90	11	90	90
Number of signal averages	1	4	2	3
Slices	1	7	1	1
Slice thickness/gap (mm)	2.0 / n/a	3.2 / 3.2	2.0 / n/a	2.0 / n/a
Inversion times (ms)	150, 300, 500, 800, 1000, 1300, 1500	n/a	n/a	n/a
Spin-lock durations (ms)	n/a	0, 10, 20, 30, 40	n/a	n/a
Spin-lock frequency (Hz)	n/a	500	n/a	n/a
Duration (min sec)	11 min 54 s	14 min 10 s	5 min 25 s	4 min 51 s

n/a, not applicable

Statistical analysis

Statistical analysis was done by the first and senior author (DT, SN) using Python and the numerical libraries Pandas, NumPy, and SciPy (Python Software Foundation). Mean values for T1, T1ρ, T2, and T2* were calculated for all regions and zones. Relative loading-induced changes in qMRI parameters were calculated for $\delta_{1/2}$ and δ_1, respectively, and connoted as $\Delta_{1/2}$ and Δ_1: $\Delta_{1/2} = ((qMRI\delta_{1/2} – qMRI\delta_0)/qMRI\delta_0)$ and $\Delta_1 = ((qMRI\delta_1 – qMRI\delta_0)/qMRI\delta_0)$. Normality was tested using the D'Agostino-Pearson test. As normal distributions could not be confirmed for all datasets of this study, pairwise comparisons were made using the non-parametric Wilcoxon signed-rank test. Correlations were assessed using Spearman's correlation. Data for the quantitative MRI parameters are given as medians with the corresponding interquartile ranges or Spearman's correlation coefficient ρ and *p* value. Because of the multiple variables being tested secondary to our study's exploratory nature, the Bonferroni correction was applied. The level of significance was set to $p \leq 0.05/4 = 0.0125$ as four qMRI parameters were tested which may be considered as separate experiments (in a statistical sense). No additional Bonferroni correction was performed for the distinct subregions and sub-zones to decrease the false-negative rate and preserve statistical power.

Results

Sample and patient characteristics are given in Table 2

MSS of 0, 1, 2, 3, 4, 5, 6, 7, and 8 were found in 0, 5, 9, 9, 12, 9, 9, 4, and 2 samples; therefore, the *int* group was composed of *n*int = 35 samples and the *ed* group of *n*ed = 24 samples. Median Mankin sum scores were 3 ($q_{25} = 2$, $q_{75} = 4$) in the *int* group and 6 ($q_{25} = 5$, $q_{75} = 7$) in the ed group. Median instantaneous Young's modulus in all samples was 11.73 ($q_{25} = 10.72$, $q_{75} = 13.31$) MPa and no significant differences were found between both groups (*int*, 11.66 [$q_{25} = 10.40$, $q_{75} = 12.97$] MPa; *ed*, 11.90 [$q_{25} = 11.23$, $q_{75} = 13.55$] MPa; $p = 0.82$). Median sample thickness (as determined by histology) was 2.12 ($q_{25} = 1.75$, $q_{75} = 2.49$) mm and, similarly, no significant differences were found (*int*, 1.92 [$q_{25} = 1.71$, $q_{75} = 2.50$] mm; *ed*, 2.16 [$q_{25} = 1.78$, $q_{75} = 2.44$]; $p = 0.98$).

Table 2 Sample and patient characteristics

Patients' characteristics	
Total number (samples/patients)	59/59
Sex	31 male, 28 female
Side	27 right, 32 left
Age (mean [range])	All patients, 66.0 [43–92 years]
	Male subgroup, 66.9 [51–92 years]
	Female subgroup, 65.0 [43–85 years]

Relative changes in qMRI parameters in response to loading are summarised in Table 3. Additionally, the results for the entire cartilage sample are visualised in Fig. 2. Although for T1ρ, consistent increases were found in all cartilage regions and zones, these increases were significantly higher in *ed* than in *int* samples and markedly stronger sub-pistonally (directly underneath the piston) than peri-pistonally (adjacent regions). In contrast, loading-induced changes in T1, T2, and T2* were not significantly different (Table 3).

For T1, by trend, slight decreases were found in *int* cartilage and slight increases in *ed* cartilage, yet no distinct degeneration-dependent response-to-loading patterns were discernible.

For T2, loading-induced increases were found in all samples and the increases were similarly more pronounced in *ed* than in *int* samples, yet not significant. Mean changes in T1ρ and T2 tended to be associated with loading intensity, i.e. $\Delta_1 > \Delta_{1/2}$, except for the superficial sub-pistonal region.

For T2*, loading-induced decreases were found in all samples that tended to be larger in the superficial zones and sub-pistonally.

Further analysis of $\Delta_{T1\rho}$ revealed significant correlations with the MSS; i.e. loading-induced increases in T1ρ were larger with more severe degeneration: T1ρ: Spearman's $\rho_{\delta½} = 0.35$ ($p = 0.007$); $\rho_{\delta1} = 0.31$ ($p = 0.016$) (Fig. 3). In contrast, no significant correlations between Δ_{T2}, Δ_{T2*}, Δ_{T1}, and the MSS were found.

The qualitative assessment revealed similar findings (Fig. 4): Although all samples, regardless of degeneration, displayed increases in T1ρ when loaded, these changes were considerably larger in *ed* cartilage and associated with distinctly different patterns of tissue involvement. While in *int* samples, increased signal intensities in T1ρ were primarily limited to the superficial zones and tended not to involve adjacent peri-pistonal regions; these extended throughout the entire cartilage depth and cross-sectional area in *ed* samples.

In absolute terms, qMRI parameters were not significantly different between *int* and *ed* cartilage samples except for a few significant differences in T1 at $\delta_{1/2}$ (i.e. DZ SPA and SZ PPA [$p < 0.01$]) (Table 4). In particular, no significant differences between *int* and *ed* samples were found for any qMRI parameter in the unloaded state. Moreover, no significant correlations were found between biomechanical properties and changes in qMRI parameters (Online Supplement 2).

Discussion

The most important finding of this study is that cartilage functionality assessment by T1ρ mapping provides a promising diagnostic tool to detect early and thus potentially reversible cartilage degeneration.

Table 3 Relative changes in qMRI parameters [%] in response to loading

		T1		T1ρ		T2		T2*	
		$\Delta_{½}$	Δ_1	$\Delta_{½}$	Δ_1	$\Delta_{½}$	Δ_1	$\Delta_{½}$	Δ_1
ECS	Intact	− 0.8 [− 1.5, 1.0]	− 2.2 [− 4.0, − 0.5]	12.7 [5.9, 19.5]	15.5 [7.1, 18.3]	1.8 [0.7, 5.0]	3.5 [− 0.4, 5.9]	− 7.3 [− 12.2, − 2.8]	− 7.8 [− 12.8, − 4.2]
	Early deg	− 1.2 [− 1.8, 1.2]	− 2.3 [− 4.3, − 0.5]	23.8 [18.1, 29.0]	26.1 [16.8, 32.1]	3.4 [1.1, 5.1]	4.8 [1.8, 6.1]	− 5.8 [− 9.5, − 2.4]	− 5.6 [− 8.9, − 2.2]
	p value	0.65	1.0	*< 0.001*	*< 0.001*	0.39	0.17	0.44	0.22
FT SPA	Intact	− 0.0 [− 1.6, 1.1]	− 3.0 [− 5.5, − 1.1]	14.7 [6.4, 25.0]	18.2 [10.5, 23.8]	2.4 [0.8, 6.5]	3.3 [−0.9, 6.4]	− 10.8 [− 15.7, − 4.1]	− 11.4 [− 17.4, − 5.1]
	Early deg	− 1.5 [− 2.7, 1.0]	− 3.8 [− 5.3, − 1.6]	31.4 [17.7, 34.5]	31.0 [18.5, 38.0]	3.0 [1.0, 7.0]	2.7 [0.8, 5.7]	− 7.5 [− 12.3, − 4.4]	− 9.5 [− 15.9, − 4.2]
	p value	0.35	0.69	*< 0.001*	*< 0.01*	0.57	0.88	0.35	0.71
SZ SPA	Intact	− 2.8 [− 5.7, 4.3]	− 4.6 [− 13.5, − 1.0]	12.5 [6.4, 27.8]	9.6 [1.4, 22.3]	5.3 [− 5.1, 12.6]	2.9 [− 9.0, 11.5]	− 26.7 [−37.1, − 16.2]	− 24.2 [− 35.9, − 8.8]
	Early deg	− 2.7 [− 5.6, 2.9]	− 8.0 [− 13.3, − 3.9]	28.5 [18.5, 47.9]	24.8 [14.8, 38.0]	4.5 [− 1.9, 17.7]	0.5 [− 8.4, 13.0]	− 23.5 [− 32.7, − 17.1]	− 23.8 [− 31.8, − 13.0]
	p value	0.84	0.47	*< 0.001*	*< 0.01*	0.56	0.99	0.31	0.7
TZ SPA	Intact	− 0.3 [− 1.7, 0.8]	− 2.9 [− 5.4, − 1.1]	16.8 [8.0, 27.6]	21.2 [13.8, 28.5]	2.7 [0.9, 6.7]	5.0 [− 0.6, 8.3]	− 7.3 [− 12.0, 1.0]	− 7.2 [− 13.6, − 0.8]
	Early deg	0.8 [− 2.4, 2.5]	− 0.4 [− 4.4, 1.4]	31.4 [19.5, 35.7]	31.0 [20.9, 41.5]	6.5 [1.4, 10.9]	5.4 [1.8, 12.9]	− 4.0 [− 10.3, 2.2]	− 4.1 [− 14.3, 3.6]
	p value	0.32	0.08	*< 0.01*	*0.01*	0.12	0.39	0.36	0.4
DZ SPA	Intact	1.3 [− 1.3, 3.4]	− 1.0 [− 4.4, 1.5]	13.6 [5.4, 19.4]	15.7 [6.9, 21.0]	1.3 [− 3.4, 4.8]	1.0 [− 4.0, 4.7]	− 3.4 [− 9.5, 0.9]	− 5.1 [− 11.0, − 1.3]
	Early deg	− 1.5 [− 3.4, 0.2]	− 2.8 [− 5.7, − 1.1]	25.5 [16.2, 29.4]	27.5 [20.8, 36.2]	− 0.4 [− 4.3, 3.6]	1.1 [− 4.9, 4.3]	− 4.6 [− 11.1, − 1.2]	− 7.8 [− 12.8,− 1.7]
	p value	0.04	0.16	*< 0.01*	*< 0.001*	0.37	0.98	0.73	0.42
FT PPA	Intact	− 0.7 [− 1.8, 0.7]	− 0.8 [− 2.7, 0.8]	7.4 [2.9, 11.4]	9.4 [4.0, 15.0]	1.5 [−1.0, 6.3]	2.9 [0.4, 7.1]	−2.1 [−7.3, 0.7]	− 2.0 [− 6.0, − 0.1]
	Early deg	− 0.1 [− 1.8, 1.5]	− 0.8 [− 2.0, 1.2]	21.5 [11.8, 26.3]	20.8 [15.3, 28.5]	2.4 [− 0.2, 5.1]	4.9 [1.3, 8.8]	− 1.7 [− 6.6, 2.0]	− 0.2 [− 6.5, 3.3]
	p value	0.34	0.63	*< 0.001*	*< 0.001*	0.29	0.19	0.35	0.23
SZ PPA	Intact	− 1.0 [− 3.7, 1.7]	− 1.4 [− 5.0, 0.6]	12.8 [2.7, 16.3]	11.9 [1.5, 22.2]	2.3 [− 0.7, 11.0]	7.3 [0.6, 11.0]	− 2.0 [− 11.2, 3.4]	− 1.9 [− 11.2, 3.5]
	Early deg	1.2 [− 1.4, 2.9]	− 0.3 [− 1.7, 2.0]	25.4 [12.8, 37.8]	25.2 [19.2, 34.5]	7.8 [1.9, 9.8]	8.6 [4.5, 12.8]	1.1 [− 5.8, 11.0]	3.2 [− 7.8, 9.2]
	p value	0.05	0.13	*< 0.001*	*< 0.001*	0.16	0.14	0.14	0.08
TZ PPA	Intact	− 1.1 [− 1.7, 0.6]	− 1.3 [− 2.6, 0.2]	7.3 [0.5, 12.4]	9.2 [4.5, 14.2]	1.3 [− 0.9, 6.2]	3.1 [0.2, 6.7]	− 1.5 [− 6.6, 1.8]	− 1.1 [− 6.9, 2.4]
	Early deg	− 1.2 [− 2.0, 0.8]	− 0.7 [− 3.0, 0.9]	17.0 [11.0, 23.9]	20.4 [14.5, 27.9]	1.9 [− 0.6, 6.1]	4.3 [2.3, 9.9]	− 2.2 [− 5.6, 4.5]	0.5 [− 5.6, 4.7]
	p value	0.87	0.42	*< 0.001*	*< 0.001*	0.37	0.08	0.4	0.16
DZ PPA	Intact	− 0.2 [− 3.5, 3.2]	0.3 [− 3.9, 3.5]	5.5 [0.6, 14.3]	6.7 [1.2, 13.1]	− 0.8 [− 5.6, 8.1]	0.6 [− 5.1, 6.4]	− 3.9 [− 7.6, − 0.8]	− 4.4 [− 8.4, 0.8]
	Early deg	− 0.9 [− 3.8, 2.6]	− 1.1 [− 3.8, 2.8]	18.6 [9.7, 24.0]	18.2 [11.6, 25.8]	0.3 [− 3.0, 3.3]	− 0.2 [− 4.0, 6.9]	− 4.3 [− 9.9, − 0.0]	− 5.1 [− 9.1, 0.5]
	p value	0.88	0.83	*< 0.001*	*< 0.001*	0.85	0.79	0.91	0.84

Values are given as median [25%-quantile, 75%-quantile]. $\Delta_{½}$ and Δ_1 give the relative change in the respective qMRI parameter in response to moderate and severe loading (i.e. displacement to 405 μm or 810 μm) as referenced to the unloaded state. Intact cartilage, i.e. Mankin sum scores 0–4, vs. early degenerative cartilage (early deg), i.e. Mankin sum scores 5–8. Wilcoxon signed-rank test was used for group-wise comparisons between intact and early deg. samples; significant differences are in *italics*. *SZ*, superficial zone; *TZ*, transitional zone; *DZ*, deep zone; *FT*, full-thickness (SZ + TZ + DZ); *SPA*, sub-pistonal area; *PPA*, peri-pistonal area; *ECS*, entire cartilage sample

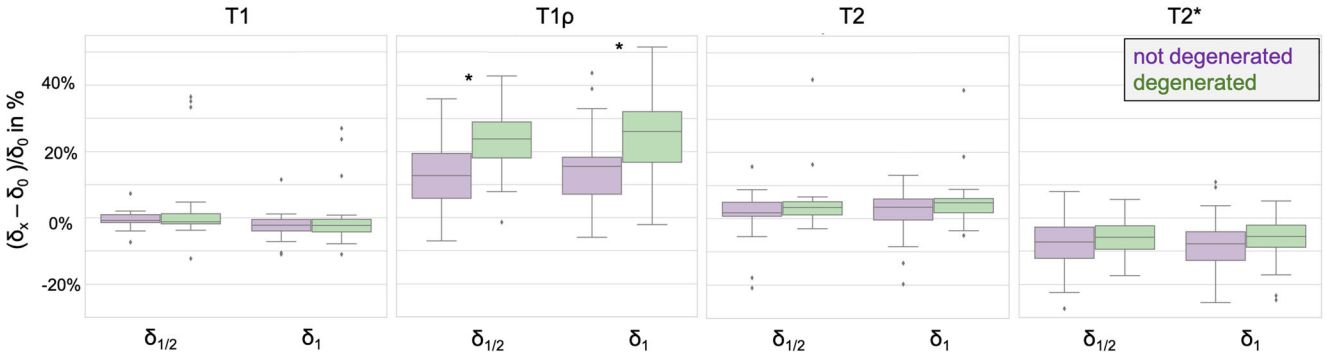

Fig. 2 Relative changes of qMRI parameters for the entire cartilage sample. Relative changes at consecutive displacement positions, i.e. $\delta_{1/2}$ and δ_1, are given against the unloaded state (δ_0) in percent. Results are shown for intact samples (purple) and early degenerated samples (green). Significant differences between the two groups were found for T1ρ, but not for T1, T2, or T2*. Please see Table 3 for details

Presumably due to the high inter- and intra-individual variability [5, 7], qMRI parameters measured statically, i.e. unloaded, per se fail to differentiate intact from early degenerative cartilage.

Building upon previous work that established the applicability of qMRI in the context of functional imaging and defined response-to-loading patterns of histologically intact cartilage samples [14], the present study demonstrates that loading-induced changes as quantified by sequential T1ρ mapping are related to histological degeneration and thereby not only provide a viable surrogate of cartilage functionality but also allow the abovementioned differentiation.

In our study, consistent loading-induced increases in T1ρ were found. The literature data are contradictory with some authors attesting disparate responses-to-loading patterns in the superficial and deep cartilage layers of the femur [10–12], while others reported decreases [9, 13] or increases [14, 18]. Although these inconsistencies may be attributed to inherent differences in loading regimens, study designs, imaging protocols, segmentation approaches, and species, qMRI-based cartilage functionality remains to be fully elucidated. Yet, one consistent finding was that larger loading-induced changes were present in osteoarthritic joints: Souza et al found an 8% significant reduction in T1ρ in the medial compartment that was more accentuated in mild OA than in healthy joints [13]. Upon further zonal assessment, they observed these reductions to be primarily due to the tibial cartilage, where decreases in T1ρ were larger in OA knees [10]. Our study is reflective thereof as increases in T1ρ were significantly greater in early degenerative than in intact cartilage. Even though

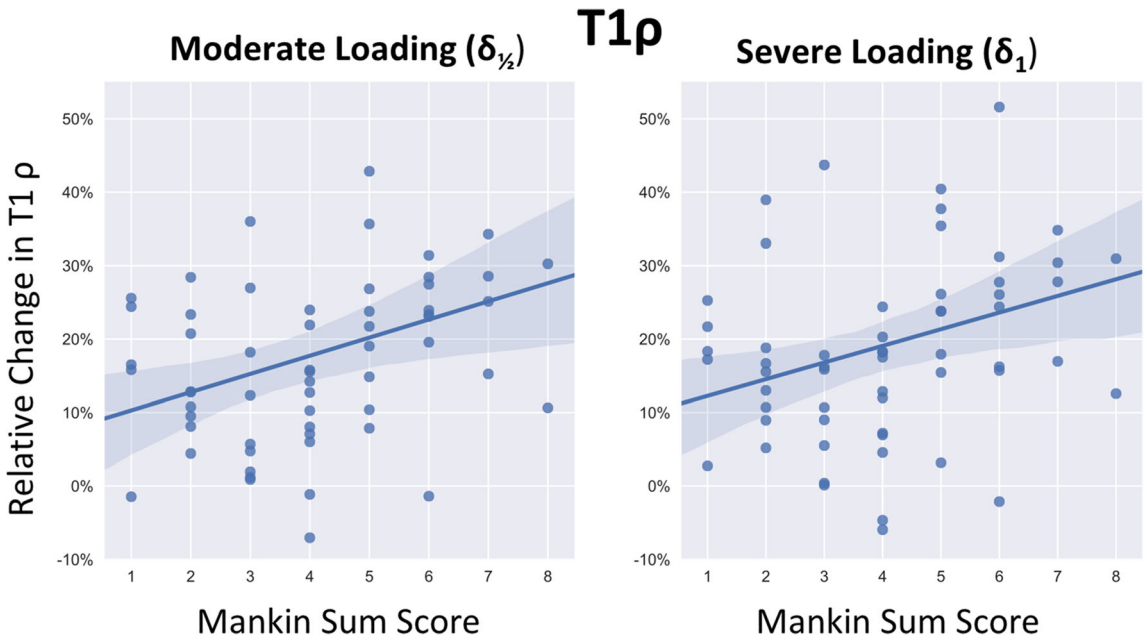

Fig. 3 Relative changes in T1ρ as a function of histological degeneration. Correlation of relative changes in T1ρ with Mankin sum scores in response to loading. Spearman's $\rho_{\delta½} = 0.35$ ($p = 0.007$); $\rho_{\delta1} = 0.31$ ($p = 0.016$). The shaded areas denote the 95% confidence interval of the regression. Segmentation included the entire cartilage cross-sectional area (ECS). $\delta_{½}$ or δ_1 indicates displacement-induced loading to 405 μm or 810 μm

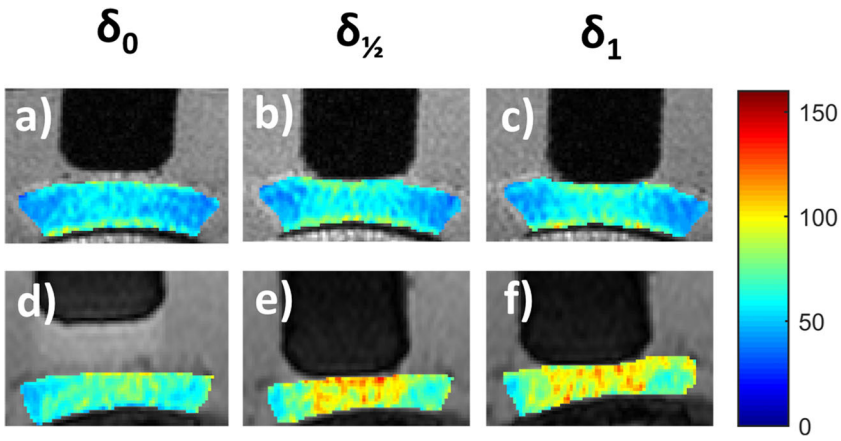

Fig. 4 Sequential T1ρ maps as a function of loading of two representative cartilage samples. T1ρ maps are displayed at consecutive indentation positions δ_0 (unloaded; **a**, **d**), $\delta_{½}$ (displacement to 405 μm; **b**, **e**), and δ_1 (displacement to 810 μm; **c**, **f**). Grossly intact (Mankin sum score 2, **a**–**c**) and early degenerative cartilage sample (Mankin sum score 7, **d**–**f**). Scale extends from 0 to 160 ms

T1ρ is not specific towards any particular cartilage constituent, let alone the tissue's proteoglycan content [21, 22], common consensus prevails that it is representative of tissue hydration [23] and a marker of biologically meaningful intra-tissue changes [18]. Mechanistically, once loaded, tissue thickness and water content are reduced, which in turn lead to a relatively increased proteoglycan concentration due to extracellular matrix condensation and deformation [24]. Also, fibre orientation relative to B_0 is altered in loaded areas where tangentially oriented fibres (present in the superficial zone) are flattened and more planar, while radially oriented fibres (transitional and deep zones) are spread out and more crimped [25]. Likewise, the number of fibres oriented at the magic angle (creating higher signal intensity) is greater than in adjacent tissue areas, which may be reflected by larger T1ρ increases in the sub-pistonal area.

So what changes in cartilage degeneration may be contributory to altered load-bearing? In early degeneration, cartilage height is lost and the proteoglycan and water fractions alongside the overall fixed-charge density are substantially decreased, whereas the collagen fraction is (relatively) increased. Superficial collagen fibrils are oriented less parallel and local tissue strains are increased throughout the tissue depth [4]. Therefore, the more pronounced changes in early degenerative cartilage have structural and compositional correlates that may be best assessed using serial T1ρ mapping.

Unexpectedly, no distinct degeneration-dependent response-to-loading patterns could be identified for T2, T2*, or T1. Although T2 is considered a marker of water content and matrix composition, no significant loading-induced differences were found as a function of degeneration. Overall, changes in T2 were comparable with those in T1ρ, yet, T2 does not seem sufficiently sensitive to loading-induced intra-tissue changes which are in line with a recent in vivo study [12].

Similarly, loading-induced changes in T2* do not seem to indicate cartilage degeneration and resultant aberrant tissue functionality. Although hypothesised to be susceptible to repetitive joint loading [26], T2* changes were similar irrespective of degeneration. Surprisingly, opposite loading-induced changes in T2* and T2 were observed which may be due to the fact that T2* captures rapidly decaying T2 signal components and is greatly affected by de-phasing effects secondary to local macro- and microscopic (i.e. inter- and intra-voxel) inhomogeneities and tissue-interface-associated susceptibilities [27] that may be altered in the loaded cartilage. In light of the technique's susceptibility to artefacts, its as yet unclear sensitivity and specificity profiles [21] and disputed correlations with histological measures [28, 29], T2* may not be useful in cartilage functionality assessment.

For T1, slight differences in loading-induced changes were identified: slight decreases in intact cartilage and slight increases in degenerative cartilage. Not least due to the substantial standard deviation, these findings were not significant, yet T1 mapping of native cartilage has been demonstrated before to be indicative of loading-induced intra-tissue changes [30] and may therefore be considered an ancillary parameter of cartilage functionality. Yet, undoubtedly, the clinical potential of T1 lies with the dGEMRIC technique (delayed gadolinium-enhanced MRI of cartilage) and the presence of gadolinium, which was not assessed in this study. No significant degeneration-dependent differences in the biomechanical properties were observed, which is mainly due to the great overlap in biomechanical measures of healthy and degenerative cartilage [31] and the fact that biomechanical properties are mainly determined by matrix integrity rather than its composition [32]. Correspondingly, no significant differences in the qMRI parameters in the unloaded state were found.

Limitations involve technical and biological issues. First, indentation loading by control of displacement brings about variable intra-tissue strains depending on sample thickness, thereby limiting inter- and intra-sample comparability. Future studies should therefore use force-controlled indentation loading devices to achieve more standardised loading, even when applying lengthy scan protocols [15]. Second, cartilage experiences a combination of compression and shearing when load-bearing under physiological conditions [33], which

Table 4 Absolute qMRI parameter values (ms) in response to indentation loading

		T1			T1ρ			T2			T2*		
		δ_0	$\delta_{½}$	δ_1	δ_0	$\delta_{½}$	δ_1	δ_0	$\delta_{½}$	δ_1	δ_0	$\delta_{½}$	δ_1
ECS	Intact	668.7 [625.2, 747.1]	668.5 [604.9, 744.2]	653.3 [591.8, 729.9]	59.5 [45.8, 76.5]	71.4 [49.6, 85.6]	71.1 [51.0, 89.4]	32.0 [28.0, 41.1]	31.7 [27.8, 42.5]	32.1 [27.9, 43.0]	26.3 [22.3, 32.5]	24.2 [21.3, 30.8]	24.3 [21.4, 30.3]
	Early deg	732.6 [686.6, 774.6]	734.4 [692.0, 781.3]	708.6 [658.1, 752.0]	60.3 [50.4, 67.4]	78.1 [65.4, 88.2]	76.5 [65.0, 88.4]	33.0 [31.2, 39.0]	34.3 [32.4, 42.1]	34.6 [32.8, 42.6]	27.2 [25.3, 33.4]	26.5 [23.7, 30.1]	26.4 [23.8, 30.8]
	p value	*0.02*	*< 0.01*	0.02	0.91	0.22	0.27	0.33	0.13	0.09	0.25	0.15	0.15
FT SPA	Intact	658.1 [623.8, 722.3]	666.3 [610.3, 735.8]	644.4 [585.6, 716.3]	64.7 [47.7, 80.6]	74.9 [53.4, 93.5]	79.0 [54.9, 98.2]	31.6 [27.5, 40.8]	32.3 [28.0, 42.2]	32.5 [28.0, 43.5]	27.4 [22.9, 32.4]	24.2 [21.0, 30.0]	24.0 [21.1, 30.0]
	Early deg	723.4 [682.0, 782.4]	737.8 [691.1, 762.8]	706.0 [639.3, 741.3]	63.9 [54.1, 72.2]	83.2 [70.9, 94.8]	83.4 [69.7, 98.2]	32.5 [31.0, 38.8]	34.5 [32.2, 43.8]	34.0 [32.2, 43.1]	27.7 [26.1, 34.7]	26.0 [23.7, 31.2]	25.3 [22.4, 31.5]
	p value	*< 0.01*	*< 0.01*	0.03	0.98	0.19	0.23	0.33	0.11	0.2	0.25	0.12	0.32
SZ SPA	Intact	722.4 [633.4, 803.6]	701.4 [630.8, 807.8]	664.9 [598.0, 731.8]	75.6 [56.4, 103.1]	91.2 [63.2, 109.9]	88.2 [61.7, 113.5]	37.4 [27.6, 49.4]	38.7 [29.7, 47.6]	33.7 [30.2, 47.5]	29.3 [26.1, 38.8]	21.7 [19.9, 25.5]	22.2 [20.0, 24.8]
	Early deg	793.9 [705.3, 823.3]	762.1 [682.1, 852.3]	680.4 [654.5, 731.6]	71.7 [63.7, 85.0]	99.4 [85.9, 117.4]	91.4 [80.4, 116.4]	36.6 [32.2, 47.5]	42.9 [36.1, 48.2]	40.0 [34.5, 46.8]	31.4 [27.6, 35.3]	22.8 [21.0, 26.5]	22.4 [20.9, 25.5]
	p value	0.11	0.05	0.18	0.85	0.19	0.31	0.59	0.25	0.37	0.51	0.25	0.36
TZ SPA	Intact	686.3 [635.3, 772.0]	689.2 [631.5, 773.4]	676.2 [613.3, 753.1]	64.8 [45.9, 79.3]	75.9 [51.3, 92.0]	81.0 [53.9, 98.9]	33.6 [27.3, 45.4]	34.6 [28.9, 47.2]	34.6 [30.4, 49.1]	29.4 [22.3, 36.1]	26.3 [21.7, 34.1]	26.1 [21.6, 34.1]
	Early deg	750.3 [733.2, 813.7]	773.8 [731.8, 800.8]	750.0 [680.5, 790.6]	63.2 [51.7, 69.7]	81.8 [67.2, 92.1]	81.8 [66.9, 97.3]	33.7 [31.3, 42.3]	35.7 [33.2, 45.5]	36.1 [32.9, 47.2]	27.9 [25.9, 36.3]	28.4 [24.6, 34.1]	27.2 [23.8, 35.9]
	p value	0.03	0.01	0.02	1.0	0.24	0.36	0.6	0.22	0.44	0.49	0.19	0.34
DZ SPA	Intact	569.3 [522.6, 637.8]	569.9 [527.7, 619.1]	579.0 [511.9, 611.0]	60.1 [49.8, 74.6]	70.6 [51.6, 82.8]	71.4 [48.2, 86.5]	27.1 [22.9, 35.6]	26.8 [22.9, 33.8]	27.1 [23.7, 34.0]	22.4 [20.4, 27.6]	22.1 [19.1, 25.3]	22.6 [19.2, 25.7]
	Early deg	649.7 [581.8, 695.4]	626.4 [592.9, 681.3]	616.0 [554.5, 659.4]	59.3 [53.6, 70.9]	73.1 [66.7, 88.9]	78.2 [65.9, 92.6]	28.6 [26.7, 32.2]	29.3 [26.2, 32.5]	30.9 [26.1, 34.8]	24.2 [22.7, 27.6]	23.7 [22.3, 26.2]	23.3 [20.7, 25.9]
	p value	0.01	*< 0.01*	0.03	0.71	0.09	0.08	0.18	0.15	0.16	0.14	0.11	0.28
FT PPA	Intact	682.8 [624.5, 757.7]	672.9 [627.8, 750.0]	671.3 [620.1, 740.1]	55.4 [40.5, 73.6]	66.8 [42.2, 79.1]	62.5 [44.1, 82.5]	33.1 [27.7, 41.7]	33.3 [27.9, 42.5]	31.7 [28.0, 43.5]	25.3 [21.9, 32.7]	24.6 [21.2, 31.5]	24.3 [21.2, 29.0]
	Early deg	714.2 [685.4, 764.0]	724.0 [674.5, 770.1]	713.8 [667.8, 757.4]	56.9 [47.8, 64.7]	69.2 [59.0, 80.5]	69.3 [56.4, 83.9]	33.5 [30.3, 40.1]	34.4 [32.5, 41.3]	35.2 [32.1, 42.2]	26.1 [25.2, 31.9]	27.0 [23.7, 30.3]	27.1 [24.6, 30.8]
	p value	0.05	0.02	0.06	0.58	0.29	0.26	0.28	0.2	0.28	0.14	0.21	0.09
SZ PPA	Intact	726.8 [666.8, 778.1]	706.2 [655.0, 780.3]	713.8 [655.0, 774.1]	61.8 [43.0, 89.1]	75.4 [45.4, 93.0]	76.1 [49.2, 96.8]	34.5 [29.7, 49.3]	35.9 [29.9, 49.5]	35.4 [30.5, 52.6]	28.0 [23.6, 33.3]	27.3 [22.1, 32.7]	25.6 [22.6, 31.7]
	early deg	773.5 [719.7, 803.4]	788.4 [731.4, 828.2]	790.7 [705.2, 811.5]	63.3 [51.9,7 0.5]	76.7 [67.9, 95.5]	79.1 [63.6, 94.0]	38.2 [32.6, 41.1]	39.8 [35.0, 45.3]	41.2 [36.2, 46.7]	29.1 [24.9, 33.7]	28.0 [25.0, 34.2]	28.6 [24.5, 33.6]
	p value	0.04	*< 0.01*	0.02	0.68	0.27	0.38	0.21	0.24	0.17	0.29	0.46	0.32
TZ PPA	Intact	700.6 [640.8, 791.1]	707.5 [639.6, 777.2]	697.5 [639.8, 768.6]	54.6 [38.6, 70.3]	63.6 [39.9, 74.8]	60.9 [42.5, 79.9]	33.2 [28.6, 44.3]	33.7 [28.5, 47.3]	34.2 [28.2, 47.1]	25.6 [21.5, 34.3]	24.9 [21.0, 33.0]	24.0 [21.1, 29.4]
	Early deg	759.5 [721.4, 795.1]	759.2 [712.8, 801.0]	751.8 [704.6, 805.4]	53.9 [47.3, 63.2]	63.9 [54.1, 76.8]	65.6 [54.4, 82.9]	34.5 [30.8, 41.9]	35.1 [32.6, 42.9]	35.4 [34.1, 45.0]	27.0 [25.0, 32.5]	27.6 [23.8, 31.5]	28.1 [25.8, 32.4]
	p value	0.06	0.04	0.04	0.51	0.27	0.12	0.45	0.31	0.22	0.16	0.22	0.02
DZ PPA	Intact	570.1 [525.5, 655.1]	578.1 [519.5, 644.5]	572.2 [517.2, 653.9]	55.5 [42.7, 69.5]	61.7 [44.7, 76.4]	62.5 [42.8, 76.7]	26.3 [22.5, 33.2]	25.5 [23.1, 33.4]	26.6 [23.0, 34.3]	22.5 [18.9, 25.4]	21.3 [19.3, 24.4]	21.0 [19.3, 25.0]
	Early deg	653.3 [582.6, 696.6]	628.0 [587.7, 688.1]	608.9 [572.7, 681.6]	55.7 [46.5, 64.5]	69.0 [60.0, 76.3]	65.4 [59.4, 78.0]	29.1 [27.2, 32.3]	29.4 [27.9, 33.1]	29.3 [27.7, 33.6]	25.1 [21.8, 25.6]	22.9 [21.5, 25.0]	23.3 [22.0, 24.8]
	p value	0.04	0.01	0.06	0.56	0.09	0.15	0.12	0.03	0.09	0.05	0.07	0.07

Values are given as median [25%-quantile, 75%-quantile]. δ_0, $\delta_{1/2}$, and δ_1 give the absolute qMRI parameter as measured in the unloaded configuration (i.e. δ_0) and in response to moderate and severe loading (i.e. displacement to 405 μm [$\delta_{1/2}$] and 810 μm [δ_1]). Intact cartilage, i.e. Mankin sum scores 0–4, vs. early degenerative cartilage (early deg), i.e. Mankin sum scores 5–8. Wilcoxon signed-rank test was used for group-wise comparisons between intact and early deg. samples for each loading position and qMRI parameter; significant differences are in *italics*. *SZ*, superficial zone; *TZ*, transitional zone; *DZ*, deep zone; *FT*, full thickness (SZ + TZ + DZ); *SPA*, sub-pistonal area; *PPA*, peri-pistonal area; *ECS*, entire cartilage sample

is not adequately reflected by our device and necessitates more physiological devices [15]. Third, MRI measurements per sample and indentation position lasted approximately 37 min during which time adaptive intra-tissue processes are certain to have occurred. Even though the same sequence order, i.e. T2*-T2-T1ρ-T1, was observed throughout the study, samples are likely to have experienced slightly different loading conditions with ongoing loading due to sample relaxation, thereby potentially introducing parameter drifting and inaccuracy in quantification. Nonetheless, the differences in timing are not likely to be responsible for the significant degeneration-related differences observed for T1ρ (as opposed to T2, T2*, or T1) as significant changes were found for T1ρ for both successive indentation levels. Despite our efforts for topoanatomic consistency, differences in the response-to-loading patterns reported in the literature [10, 11] and in our study may be attributed to the relative lack of shearing forces in indentation loading. Fourth, technical limitations involve image resolution that was lower for T1ρ to balance the signal-to-noise ratio and measurement duration. Maps were interpolated accordingly, which improves the apparent spatial resolution and reduces partial volume effects [34], but remains a source of inaccuracy.

One strength of our study is the use of clinically applicable qMRI sequences that render the eventual clinical translation of our results more likely. Oftentimes, ex vivo experiments use, for example, T1ρ sequences with exceedingly long spin-lock frequencies which are not feasible in vivo due to safety restrictions (i.e. concerning the specific absorption rate).

In conclusion, our study demonstrates that cartilage functionality may be assessed by functional qMRI mapping techniques to identify aberrant response-to-loading patterns as a function of degeneration. T1ρ is the most promising parameter that not only provides a quantitative biomarker of the tissue's load-bearing capacity but also helps to identify early cartilage degeneration.

Funding This study has received funding by the START programme of the Faculty of Medicine, RWTH Aachen, Germany, through means of a grant given to SN (691702) and through the START rotation programme granted to DT.

Compliance with ethical standards

Guarantor The scientific guarantor of this publication is Daniel Truhn.

Conflict of interest The authors of this manuscript declare no relationships with any companies, whose products or services may be related to the subject matter of the article.

Statistics and biometry One of the authors has significant statistical expertise.

Informed consent Written informed consent was obtained from all subjects (patients) in this study.

Ethical approval Institutional Review Board approval was obtained.

Methodology
- prospective
- experimental
- performed at one institution

References

1. Bay-Jensen AC, Hoegh-Madsen S, Dam E et al (2010) Which elements are involved in reversible and irreversible cartilage degradation in osteoarthritis? Rheumatol Int 30:435–442
2. Palmer AJ, Brown CP, McNally EG et al (2013) Non-invasive imaging of cartilage in early osteoarthritis. Bone Joint J 95-B:738–746
3. Guermazi A, Alizai H, Crema MD, Trattnig S, Regatte RR, Roemer FW (2015) Compositional MRI techniques for evaluation of cartilage degeneration in osteoarthritis. Osteoarthritis Cartilage 23:1639–1653
4. Saarakkala S, Julkunen P, Kiviranta P, Mäkitalo J, Jurvelin JS, Korhonen RK (2010) Depth-wise progression of osteoarthritis in human articular cartilage: investigation of composition, structure and biomechanics. Osteoarthritis Cartilage 18:73–81
5. Neu CP (2014) Functional imaging in OA: role of imaging in the evaluation of tissue biomechanics. Osteoarthritis Cartilage 22:1349–1359
6. Xia Y, Wang N, Lee J, Badar F (2011) Strain-dependent T1 relaxation profiles in articular cartilage by MRI at microscopic resolutions. Magn Reson Med 65:1733–1737
7. Nebelung S, Brill N, Tingart M et al (2016) Quantitative OCT and MRI biomarkers for the differentiation of cartilage degeneration. Skeletal Radiol 45:505–516
8. Shiomi T, Nishii T, Tanaka H et al (2010) Loading and knee alignment have significant influence on cartilage MRI T2 in porcine knee joints. Osteoarthritis Cartilage 18:902–908
9. Hamada H, Nishii T, Tamura S, Tanaka H, Wakayama T, Sugano N (2015) Comparison of load responsiveness of cartilage T1rho and T2 in porcine knee joints: an experimental loading MRI study. Osteoarthritis Cartilage 23:1776–1779
10. Souza RB, Kumar D, Calixto N et al (2014) Response of knee cartilage T1rho and T2 relaxation times to in vivo mechanical loading in individuals with and without knee osteoarthritis. Osteoarthritis Cartilage 22:1367–1376
11. Subburaj K, Souza RB, Stehling C et al (2012) Association of MR relaxation and cartilage deformation in knee osteoarthritis. J Orthop Res 30:919–926
12. Lange T, Knowles BR, Herbst M, Izadpanah K, Zaitsev M (2017) Comparative T2 and T1rho mapping of patellofemoral cartilage under in situ mechanical loading with prospective motion correction. J Magn Reson Imaging 46:452–460
13. Souza RB, Stehling C, Wyman BT et al (2010) The effects of acute loading on T1rho and T2 relaxation times of tibiofemoral articular cartilage. Osteoarthritis Cartilage 18:1557–1563
14. Nebelung S, Sondern B, Oehrl S et al (2017) Functional MR imaging mapping of human articular cartilage response to loading. Radiology 282:464–474
15. Nebelung S, Post M, Raith S et al (2017) Functional in situ assessment of human articular cartilage using MRI: a whole-knee joint loading device. Biomech Model Mechanobiol 16:1971–1986. https://doi.org/10.1007/s10237-017-0932-4
16. Cameron ML, Briggs KK, Steadman JR (2003) Reproducibility and reliability of the outerbridge classification for grading chondral lesions of the knee arthroscopically. Am J Sports Med 31:83–86

17. Nebelung S, Brill N, Müller F et al (2016) Towards optical coherence tomography-based elastographic evaluation of human cartilage. J Mech Behav Biomed Mater 56:106–119
18. Nebelung S, Sondern B, Jahr H et al (2018) Non-invasive T1rho mapping of the human cartilage response to loading and unloading. Osteoarthritis Cartilage 26:236–244
19. Mankin HJ, Dorfman H, Lippiello L, Zarins A (1971) Biochemical and metabolic abnormalities in articular cartilage from osteoarthritic human hips. II. Correlation of morphology with biochemical and metabolic data. J Bone Joint Surg Am 53:523–537
20. Gahunia HK, Lemaire C, Babyn PS, Cross AR, Kessler MJ, Pritzker KP (1995) Osteoarthritis in rhesus macaque knee joint: quantitative magnetic resonance imaging tissue characterization of articular cartilage. J Rheumatol 22:1747–1756
21. Thuring J, Linka K, Itskov M et al (2018) Multiparametric MRI and computational modelling in the assessment of human articular cartilage properties: a comprehensive approach. Biomed Res Int 2018:9460456
22. van Tiel J, Kotek G, Reijman M et al (2016) Is T1rho mapping an alternative to delayed gadolinium-enhanced MR imaging of cartilage in the assessment of sulphated glycosaminoglycan content in human osteoarthritic knees? An in vivo validation study. Radiology 279:523–531
23. Li X, Cheng J, Lin K et al (2011) Quantitative MRI using T1rho and T2 in human osteoarthritic cartilage specimens: correlation with biochemical measurements and histology. Magn Reson Imaging 29:324–334
24. Gründer W, Kanowski M, Wagner M, Werner A (2000) Visualization of pressure distribution within loaded joint cartilage by application of angle-sensitive NMR microscopy. Magn Reson Med 43:884–891
25. Gründer W (2006) MRI assessment of cartilage ultrastructure. NMR Biomed 19:855–876
26. Hesper T, Miese FR, Hosalkar HS et al (2015) Quantitative T2(*) assessment of knee joint cartilage after running a marathon. Eur J Radiol 84:284–289
27. Chavhan GB, Babyn PS, Thomas B, Shroff MM, Haacke EM (2009) Principles, techniques, and applications of T2*-based MR imaging and its special applications. Radiographics 29:1433–1449
28. Kim T, Min BH, Yoon SH et al (2014) An in vitro comparative study of T2 and T2* mappings of human articular cartilage at 3-Tesla MRI using histology as the standard of reference. Skeletal Radiol 43:947–954
29. Bittersohl B, Hosalkar HS, Miese FR et al (2015) Zonal T2* and T1Gd assessment of knee joint cartilage in various histological grades of cartilage degeneration: an observational in vitro study. BMJ Open 5:e006895
30. Xia Y, Wang N, Lee J, Badar F (2011) Strain-dependent T1 relaxation profiles in articular cartilage by MRI at microscopic resolutions. Magn Reson Med 65(6):1733–1737. https://doi.org/10.1002/mrm.22933
31. Kleemann RU, Krocker D, Cedraro A, Tuischer J, Duda GN (2005) Altered cartilage mechanics and histology in knee osteoarthritis: relation to clinical assessment (ICRS grade). Osteoarthritis Cartilage 13:958–963
32. Franz T, Hasler EM, Hagg R, Weiler C, Jakob RP, Mainil-Varlet P (2001) In situ compressive stiffness, biochemical composition, and structural integrity of articular cartilage of the human knee joint. Osteoarthritis Cartilage 9:582–592
33. Chan DD, Cai L, Butz KD, Trippel SB, Nauman EA, Neu CP (2016) In vivo articular cartilage deformation: noninvasive quantification of intratissue strain during joint contact in the human knee. Sci Rep 6:19220
34. Du YP, Parker DL, Davis WL, Cao G (1994) Reduction of partial-volume artifacts with zero-filled interpolation in three-dimensional MR angiography. J Magn Reson Imaging 4:733–741